Eur Radiol (2006) 16: 852–865
DOI 10.1007/s00330-005-0028-x



**Vincenzo Russo**
**Matteo Renzulli**
**Katia Buttazzi**
**Rossella Fattori**

# Acquired diseases of the thoracic aorta: role of MRI and MRA

Received: 19 August 2005
Accepted: 1 September 2005
Published online: 13 October 2005


V. Russo (✉) · M. Renzulli · K. Buttazzi · R. Fattori
Department of Radiology, Cardiovascular Unit, Policlinico S. Orsola, Padiglione 21, Via Massarenti 9, 40131 Bologna, Italy
e-mail: virusso@fastwebnet.it
Tel.: +39-051-6364747
Fax: +39-051-6364747

**Abstract** Diseases of the thoracic aorta can present with a broad clinical spectrum of symptoms and signs. Their prevalence appears to be increasing in western populations, most likely corresponding to aging and heightened clinical awareness but also influenced by the progress of high-resolution, noninvasive imaging modalities. Among them, MRI provides an excellent visualization of vascular structures and is well suited for evaluation of thoracic aorta disease. Currently, in many centers, noninvasive imaging modalities are the first choice in the cardiovascular system evaluation and diagnosis, reserving conventional angiography for use only before therapeutic intervention. Understanding the principle MRA techniques is essential for acquiring consistent diagnostic images. Basic technical considerations, which include fast spin-echo, fast gradient-echo, and MRA techniques with phase contrast and contrast-enhanced methods, are discussed and applied in the evaluation of acquired thoracic aorta diseases.

**Keywords** Acquired diseases · Thoracic aorta · Magnetic resonance

## Introduction

In the past few years, considerable interest in aortic diseases has been reflected in medical literature. The prevalence of aortic disease appears to be increasing in western populations, most likely corresponding to aging in addition to heightened clinical awareness. Molecular and cellular studies have elucidated the mechanisms of many pathologic conditions of the aorta and the complex interaction of this vessel with the cardiovascular system. However, increased clinical observation of aortic diseases and a more appropriate definition of its pathological substrate may also reflect concurrent outstanding progress in imaging techniques. Among the imaging modalities, MRI probably offers the greatest versatility.

With its ability to delineate the intrinsic contrast between blood flow and vessel wall, and acquire images in multiple planes with a wide field of view, MRI provides a high degree of reliability in the diagnosis of aortic diseases. MRI is totally noninvasive and can be repeated so that the progression of the disease over time can be evaluated. Functional information by dynamic sequences expands our knowledge of aortic function. MRA techniques have enhanced the noninvasive evaluation of vascular structures, making, in many instances, conventional angiography an obsolete procedure for the detection of aortic diseases.

## MRI techniques

### Spin echo MRI

Spin-echo T1-weighted imaging provides the best anatomic detail of the aortic wall and pathologic conditions such as atheromatous plaques, intimal flaps or intramural hemorrhage (Fig. 1), and is still the basis of any aortic study [1, 2], while T2-weighted images (TR, 2/3 R-R′; TE, 80–100 ms) can be used in tissue characterization of the aortic wall or blood components. Electrocardiographic (ECG) triggering is essential in minimizing motion and pulsatility artifacts. Slice thickness of 3–8 mm and an echo time (TE) of 20–30 ms are standard, while repetition time (TR) is

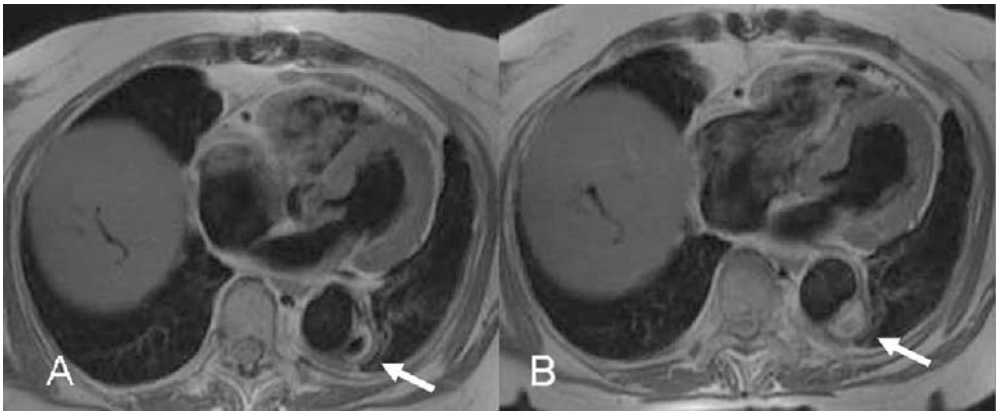


**Fig. 1** Fast spin-echo axial images of a large atheromatous plaque with a penetrating ulcer of the descending aorta (*arrows*)

determined from the R-R′ interval of the ECG. A shorter acquisition time can be achieved with fast spin-echo pulse sequences whereby a long train of echoes is acquired by using a series of 180° radiofrequency (RF) pulses; washout effects are even more substantial than conventional spin-echo techniques. A superior black-blood effect is achieved by using preparatory pulses [3] (such as presaturation, dephasing gradients, and preinversion) with one or more additional RF pulses outside the plane to suppress the signal intensity of in-flowing blood and nullify the blood signal. Therefore, "black blood" fast T1- and T2-weighted spin-echo sequences have improved image quality, with substantial saving of time and constitute, at present, the method of choice for morphologic assessment of the thoracic aorta.

Usually a conventional study of the thoracic aorta is first acquired in the axial plane, displaying the orientation of the great arteries and optimal visualization of mural lesions perpendicular to their long axes. Images in additional planes, the oblique sagittal or coronal view, are then acquired, depending on the anatomy and diagnostic problems, in order to define the longitudinal extent of the disease.

## Gradient echo MRI

Gradient-echo techniques provide dynamic and functional information, although with fewer details of the vessel wall. The bright signal of the blood pool on gradient-echo images results from flow-related enhancement obtained by applying RF pulses to saturate a volume of tissue. With a short TR (4–8 ms) and low flip angle (20–30°), maximal signal is emitted by blood flowing in the voxel. An ECG signal is acquired with the imaging data so that the images, acquired with a high degree of temporal resolution throughout the cardiac cycle (up to 20–25 frames), are reconstructed in the different phases of the cardiac cycle and can be displayed in cine format. Flow-related enhancement is produced by inflow of unsaturated blood exposed to only one RF pulse. As result, the laminar moving blood displays a bright signal in contrast to stationary tissues. The signal can be reduced if the flow is low, as in aortic aneurysms. Mural thrombi can be identified by persistent low-signal intensity in different phases of the cardiac cycle. Turbulent flow produces rapid spin dephasing and results in a signal void, providing additional information in many pathologic conditions such as coarctation, aortic valve insufficiency, aortic aneurysm, and dissection [4]. Particularly in aortic dissection, the detection of entry and re-entry sites is a special capability of functional MRI that can be helpful in planning both surgical and endovascular therapy.

## Flow mapping

Accurate quantitative information on blood flow is obtained from modified gradient-echo sequences with parameter reconstruction from the phase rather than the amplitude of the MR signal; also known as flow mapping or phase contrast or velocity-encoded cine MRI [5–7]. In each pixel of velocity images, the phase of the signal is related to the velocity component in the direction of a bipolar velocity phase-encoding gradient. In the phase image, the velocity of blood flow can be determined for any site of the vascular system. Flow velocity is calculated using a formula in which velocity is proportional to change in the phase angle of protons in motion. MR maps of flow velocity are obtained two-dimensionally, which is particularly important in profiles of nonuniform flow such as that in the great vessels. On phase images, the gray value of a pixel depends on the velocity and direction with respect to the imaging plane. Signals below a defined range are considered noise and are eliminated by a subtraction process. Quantitative data on flow velocity and flow volume are obtained from the velocity maps through a region of interest (ROI). The mean blood flow is estimated by multiplying the spatial mean velocity and the cross-sectional area of the vessel. Vector mapping has been used to describe flow patterns in different aortic diseases (e.g.,

hypertension, aneurysms, dissection Marfan syndrome, coarctation) [8–10].

### MRA

A variety of MRA techniques, including various pulse sequences, methods of data acquisition, and postprocessing have been developed in the evaluation of vascular structures [11]. However, after the introduction of faster gradient systems, 3D contrast-enhanced MRA [12–18] constitutes the method of choice for the evaluation of the aorta. The technique relies on the contrast-induced T1-shortening effects of the contrast medium whereby saturation problems with slow flow or turbulence-induced signal voids are avoided. During the short intravascular phase, the paramagnetic contrast agent provides a signal in the arterial or venous system, enhancing the vessel-to-background contrast-to-noise ratio irrespective of flow patterns and velocity. Pulsatility artifacts are minimized, even in the ascending aorta and without ECG gating. The paramagnetic contrast agent (0.2 mmol/kg of bodyweight) is generally administered i.v. (antecubital vein). Bolus timing is necessary to ensure peak enhancement during the middle of MR acquisition. The flow rate should be adjusted to guarantee that the contrast volume is injected in a period not exceeding the acquisition time, and the start delay can be easily monitored by a real-time fluoroscopic triggering when a power injector is employed [19]. Improved gradient systems allow a considerable reduction of the minimum TRs and TEs and the acquisition of complex 3D data sets within a breath-hold interval of under 30 s. With the support of MIP images andthe 3D multiplanar reformation (MPR), this technique delineates all the morphologic details of the aorta and its side branches in any plane in a 3D format (Fig. 2).

**Fig. 2** Gadolinium-enhanced 3D MRA of the thoracic aorta (surface-shaded display algorithm)

## Acquired diseases of thoracic aorta

### Aortic dissection

Aortic dissection is characterized by a laceration of the aortic intima and inner layer of the aortic media that allows blood to course through a false lumen in the outer third of the media. Dissection can occur throughout the length of the aorta. The most two common classifications (De Bakey and Stanford) are based on the anatomic location and extension of intimal flap. The most used is the Stanford one which classifies an aortic dissection irrespective of the site of the entry tear as type A if the ascending aorta is involved, and as type B if the ascending aorta is spared. Acute aortic dissection is a life-threatening condition requiring prompt diagnosis and treatment [20]. The 14-day period after onset has been designated as an acute phase because the rates of morbidity and mortality are highest during this period: 1–2% per hour in the first 24 h after onset and 80% within 2 weeks. Early and accurate detection of the dissection and a delineation of its anatomic details are critical for successful management, even if (because physical findings may be absent or may mimic other disorders such as myocardial ischemia and stroke) the diagnosis is often missed at initial evaluation [21, 22]. Thus, in dissection, the diagnostic goal is a clear anatomic delineation not only of the intimal flap and its extension, but also the detection of the entry and re-entry sites and the presence and degree of aortic insufficiency and flow in the aortic branches [23]. The relationship between true and false lumina and the visceral vessels, with any involvement of the iliac arteries and the identification of the entry and re-entry sites, are crucial in patient selection for transcatheter endovascular repair of type B acute and chronic aortic dissection [24, 25] as an alternative to open surgery (Fig. 3).

In a suspected case of aortic dissection, the standard MRI examination should begin with spin-echo “black blood” sequences. In the axial plane, the intimal flap is detected as a straight linear image inside the aortic lumen. The true lumen can be differentiated from the false by the anatomic features and flow pattern: the true lumen shows a signal void, whereas the false lumen has a higher signal intensity. In addition, the visualization of remnants of the dissected media as cobwebs adjacent to the outer wall of the lumen may help to identify the false lumen. The leakage of blood from the descending aorta into the periaortic space, which can appear with high signal intensity and result in a left-sided pleural effusion, is usually better


**Fig. 3** **a** Spin-echo sagittal image of type B dissection: the double aortic lumen is 4 cm below the left subclavian artery. The false lumen (high signal intensity) is severely dilated. **b** MRA of the same patient after stent graft treatment (*arrow*): aortic remodeling with complete thrombosis of the false lumen. The metallic structure of the stent graft produces minimal artifacts in the upper portion of the descending aorta

visualized on axial images. A high signal intensity of a pericardial effusion indicates a bloody component and is considered to be a sign of impending rupture of the ascending aorta into the pericardial space. A detailed anatomic map of aortic dissection must indicate the type and extension of dissection and distinguish the origin and perfusion of branch vessels (arch branches, celiac, superior mesenteric, renal arteries, and coronary arteries) from the true or false channels. Therefore, a further spin-echo sequence on the sagittal plane should be performed (Fig. 4) and, in stable patients, adjunctive gradient-echo sequences or phase contrast images can be instrumental in identifying aortic insufficiency and entry or re-entry sites (Fig. 5) as well as in differentiating slow flow from thrombus in the

**Fig. 4** Spin-echo sagittal image of type A dissection: the intimal flap is visible as a subtle linear image in the ascending and descending aorta

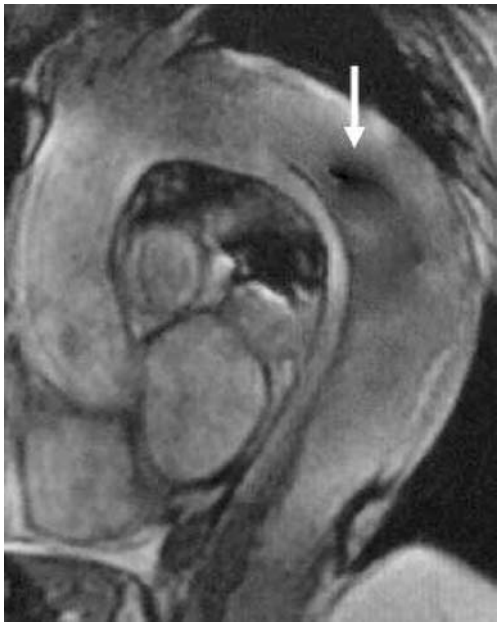

**Fig. 5** Gradient-echo sagittal image of type B dissection: flow turbulence (signal void, *arrow*) in the descending aorta indicates the entry site

**Fig. 6** MRA of aortic dissection (abdominal aorta): celiac and mesenteric arteries originate from the anterior true lumen

false lumen [26, 27]. The third step in the diagnosis of aortic dissection and definition of its anatomic detail relies on the use of Gadolinium-enhanced 3D MRA. Because 3D MRA is rapidly acquired without any need of ECG triggering and gadolinium is not nephrotoxic and causes no adverse effects, this technique may even be used with severely ill patients [28]. With spin-echo sequences, artifacts caused by imperfect ECG gating, respiratory motion or slow blood pool can result in intraluminal signal, simulating or obscuring an intimal flap. In Gadolinium-enhanced 3D MRA, the intimal flap is easily detected and the relationship with aortic vessels clearly depicted (Figs. 6, 7). Entry and re-entry sites appear as a segmental interruption of the linear intimal flap on axial or sagittal images (Fig. 8). The analysis of MRA images should not be limited to viewing MIP images or surface-shaded display (SSD); it should also include a complete evaluation of reformatted images in all three planes in order to confirm or improve spin-echo information and exclude artifacts. Combining the spin-echo with MRA images completes the diagnosis and anatomical definition [29].

At present, MRI is one of the most accurate tools in the detection of aortic dissection. A high degree of spatial resolution and contrast and the capability for multiplanar acquisition provide excellent sensitivity and specificity rating at approximately 100% in the published series [29–32].

## Intramural hematoma

Intramural hematoma (IMH) was first described in 1920 as "dissection without intimal tear" [33], but it was rarely recognized in the clinical setting before the advent of high-resolution imaging modalities. Spontaneous rupture of aortic vasa vasorum of the media layer is considered to be the initiating process, which is confined in the aortic wall without intimal tear. This results in a circumferentially oriented blood-containing space as seen in tomographic imaging studies. Although IMH may occur spontaneously or as a consequence of penetrating aortic ulcer (PAU) in intrinsically diseased media; it has also been described

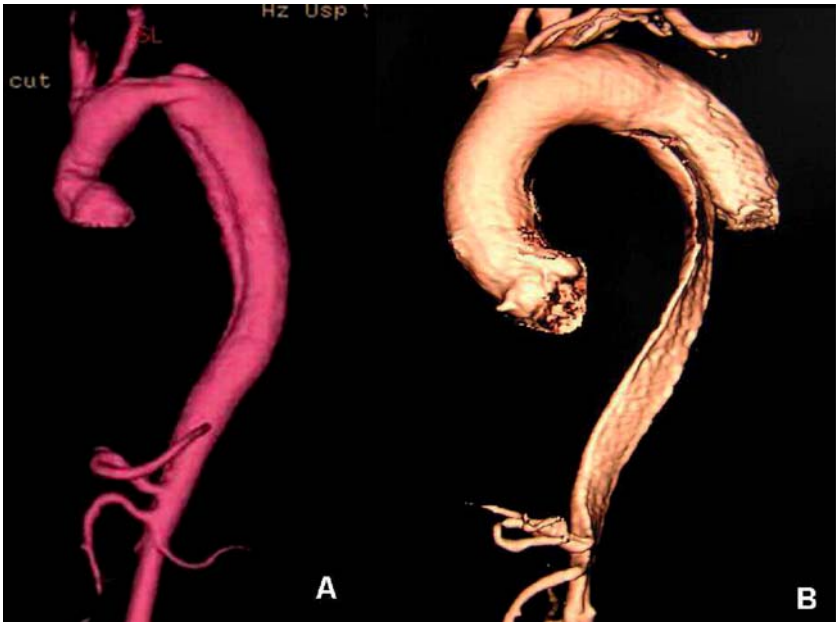


**Fig. 7** 3D MRA of aortic dissection; the false lumen is patent in A (patient with a prosthetic tube in the ascending aorta) and partially thrombosed in B

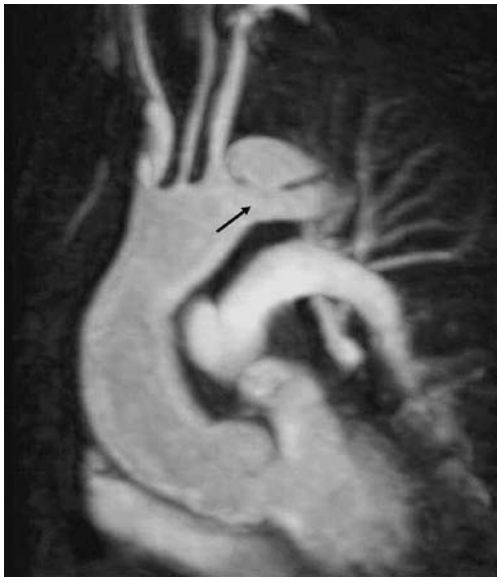

**Fig. 8** MRA of aortic dissection (thoracic aorta): the entry site is visible after the origin of left subclavian artery (*arrow*)

following blunt chest trauma [34]. As in aortic dissection, arterial hypertension is the most frequent predisposing factor. Clinical signs and symptoms and the prognosis do not differ to classic aortic dissection, and IMH should be regarded as a variant of dissection with similar or more serious prognostic and therapeutic implications [35, 36]. Typical complications of dissection such as fluid extravasation with pericardial, pleural and periaortic hematoma or aortic rupture may occur in IMH as well, even if a complete resolution of the aortic hematoma within 1 year has been reported in literature [37].

The diagnosis of IMH relies on the visualization of intramural blood manifested as a localized thickened aortic wall. The abnormal wall thickness, symmetric or asymmetric, can vary in dimension from 3 mm to more than 1 cm. The mural involvement can encompass the entire aortic circumference. However, with all the imaging modalities, IMH can be confused with clot or plaque especially if localized in the descending aorta. In a comparison of different imaging modalities, MRI demonstrated the best sensitivity in the detection of IMH [38]. T1-weighted images reveal a crescent-shaped area of abnormal signal intensity within the aortic wall (Fig. 9). Moreover, MRI is the only imaging method which may allow the assessment of the age of hematoma on the bases of the different degradation products of hemoglobin. In the acute phase (0–7 days after the onset of symptoms) on T1-weighted spin-echo images, oxyhemoglobin shows intermediate signal intensity, whereas in the subacute phase (>8 days), methemoglobin shows high signal intensity. However, when the signal intensity is medium to low, it can be difficult to distinguish IMH from mural thrombus. T2-weighted spin-echo sequences may help in differentiating the two entities: signal intensity is high in recent hemorrhage but low in chronic thrombosis [39]. The progression of IMH to overt dissection and rupture has been reported in 32% of the cases, in particular with the involvement of ascending aorta (Fig. 10). Instability of the hematoma and recurrent bleeding which can be detected by MRI are important parameters in assessing the need for surgical repair.

## Aortic ulcers

In 1934, Shennan [40] was the first to describe penetrating atheromatous ulcers of the thoracic aorta. In elderly, hypertensive patients with severe atherosclerotic involvement of the aortic wall, usually in the descending aorta, a plaque may ulcerate into the media. Aortic ulcer is characterized by rupture of the atheromatous plaque disrupting the internal elastic lamina. Extension of the ulcerated atheroma into the media may result in an intramural hematoma or localized intramedial dissection, or the plaque may break through to the adventitia and form a saccular pseudoaneurysm. The adventitia may also rupture, in which case only the surrounding mediastinal tissues contain the hematoma.

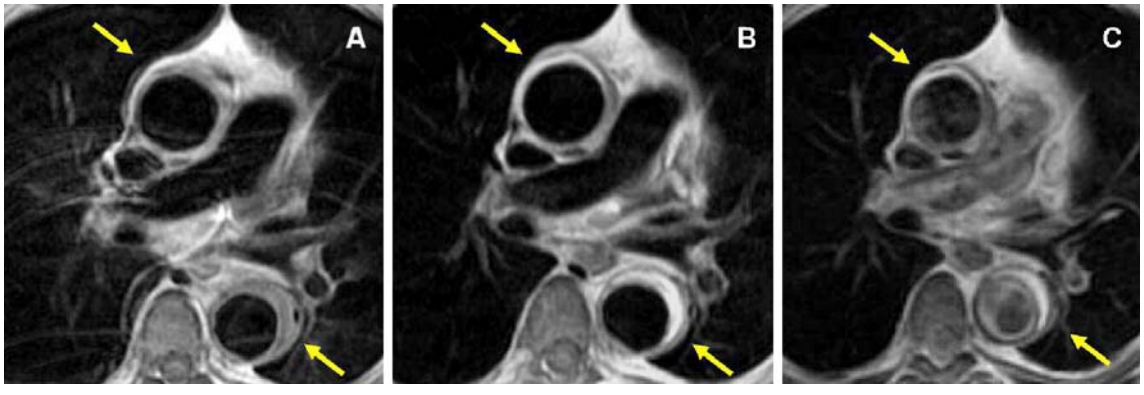


**Fig. 9** **a**, **b** T1 weighted spin-echo axial image of intramural hematoma of the ascending and descending aorta; the abnormal wall thickening (*arrows*) present intermediate signal intensity in A (oxyhemoglobin, acute phase) and high signal intensity in B (methemoglobin, subacute phase). **c** T2-weighted spin-echoimage signal intensity is high in the acute phase (recent hemorrhage)

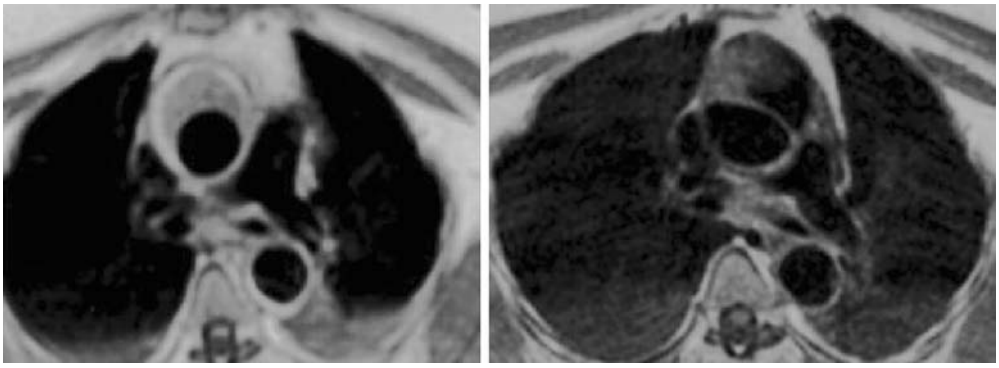

**Fig. 10** Spin-echo axial images of intramural hematoma evolved in classic dissection in the acute (**a**) and chronic (**b**) phase. **a** The high signal intensity of hematoma is visible in ascending and descending aorta. **b** Three months later the hematoma pres-ents low signal intensity and a partial area of reabsorption: an intimal flap is visible

Aortic ulcers occur almost only in the descending aorta, but location in the aortic arch or in the ascending aorta have occasionally been reported. The clinical features of penetrating atherosclerotic ulcers may be similar to those of aortic dissection, but the ulcers should be considered to be a distinct entity with a different prognosis and type of management. Persistent pain, hemodynamic instability, and signs of expansion should trigger surgical treatment, whereas asymptomatic patients can be managed medically and monitored with imaging follow-up. Incidence of transmural rupture ranging from 8 to 42% [36, 41] has been reported in medical literature. Because penetrating ulcer is much less common than classic dissection, and imaging findings may be subtle, careful awareness of its insidious behavior is particularly important for successful management.

The MRI diagnosis of aortic ulcers is based on the visualization of a crater-like ulcer located in the aortic wall (Fig. 11). Mural thickening with high or intermediate signal intensity on spin-echo sequences may indicate extension of the ulcer into the media and the formation of an intramural hematoma. MRA is particularly suitable for depicting aortic ulcers (Fig. 12) along with the irregular aortic wall profile seen in diffuse atherosclerotic involvement [42]. The aortic ulcer is easily recognized as a contrast-filled outpouching of variable extent with jagged edges, which may even result in a large pseudoaneurysm [43]. The disadvantage of MRI with respect to CT is the failure to visualize dislodgment of the intimal calcifications, frequently observed in aortic ulcers.

**Fig. 11** Spin-echo sagittal image of severe aortic atheromatous plaques and multiple penetrating ulcers of the descending aorta

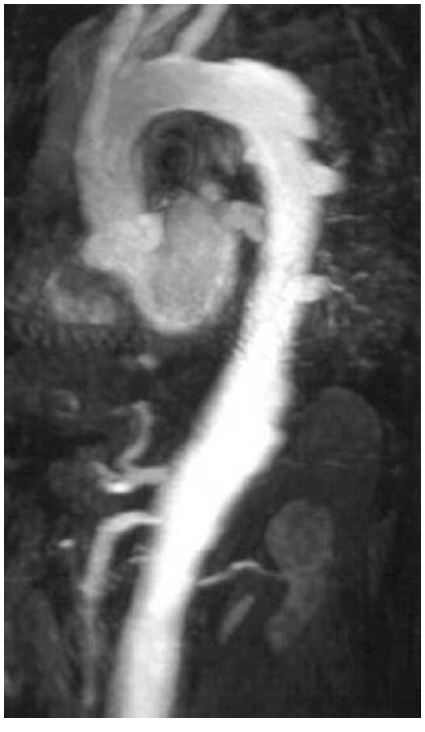

**Fig. 12** MRA of the same patient: the ulcers appear as contrast-filled outpouching protruding on the vessel profile

## Postoperative evaluation of aortic dissection

Even though early and accurate detection and an aggressive surgical approach have significantly decreased operative mortality from 40–50% to 5–7% in recent series [44, 45], patients operated for type A aortic dissection still remain at considerable risk of future complications. A persistent distal false lumen has been reported in 75–100% of the cases. Second-entry tears in the descending aorta or in the aortic arch are responsible for patency of the distal dissection, which is associated with an unfavorable prognosis. Prosthetic graft degeneration, infection (Fig. 13), or malfunction of the prosthetic aortic valves, are additional causes of postoperative complications. The reported expansion rate for dissected segments ranges between 1.2 and 4.3 mm/year. The presence of partial thrombosis of the false lumen seems to protect against dilation; an aortic growth rate of 3.4 mm/year in dissection with partial thrombosis of the false lumen versus an increase of 5.6 mm/year in dissection with no thrombosis of the false lumen has been reported [46]. Therefore, in patients who have undergone surgery for aortic dissection, an appropriate follow-up should take into account an accurate measurement of the residual aorta to identify early high-risk patients.

MRI is recognized as one of the imaging modalities of choice in postoperative evaluation [47–50]. MRI measurements are highly reproducible, and reproducibility is an essential component of serial examinations in which minimal change in dimension may represent a prognostic finding or indicate a need of preventive surgical strategies. Residual dissection is easily detected on spin-echo images, and gradient-echo sequences or phase-display images can be used to distinguish thrombosis of the false lumen from slow flow.

Slight thickening around the graft is a common finding caused by perigraft fibrosis [50, 51]. However, large or asymmetric thickening around the tube-graft may represent localized hematoma caused by an anastomotic leakage. Suture detachment with leakage has been reported, in particular after composite graft replacement of the ascending aorta. Reoperation for bleeding at the site of repair has been reported after composite graft operation in 8% of patients after 30 days and in 4% of patients after 1 year. The higher incidence of bleeding has been reported at the site of reimplanted coronary arteries. Gadolinium-enhanced MRI with standard spin-echo sequences can provide detailed information on suture detachment [52]; the site of bleeding appears as high signal intensity within the hematoma. Moreover, Gadolinium-enhanced MRA is particularly effective in the depiction of the complex postoperative anatomy and in elucidating the prosthetic tube, distal and proximal anastomoses and residual distal dissection and eventually dilated segments. Reimplanted coronary arteries or reimplanted supraaortic vessels can also be visualized by MRA and particular attention should be paid to evaluating these sites for possible postoperative weakness.

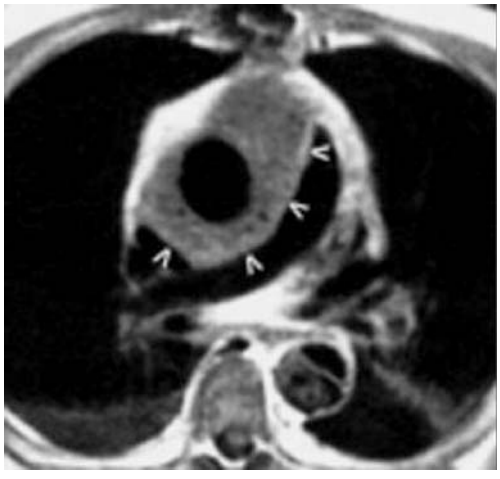

**Fig. 13** Spin-echo axial image of a periprosthetic infective collection (*arrowheads*) in a patient who underwent surgery for aortic dissection

## Thoracic aortic aneurysms

In the period between 1951 and 1980, the incidence of thoracic aortic aneurysm was estimated to be 3.5 cases per 100,000 person/year. Recently, a population-based study of thoracic and thoraco-abdominal aortic aneurysm reported an incidence of 10.9 cases per 100,000 person/year, revealing an increased rate of occurrence of the disorder [53]. Most aneurysms are atherosclerotic in nature, usually fusiform and long. Saccular false aneurysms may also develop in patients with atherosclerosis as a result of a penetrating ulcer. The natural history is quite diverse, reflecting a broad spectrum of underlying causes. Atherosclerosis is less commonly found in aneurysms of the ascending aorta than in those of the descending aorta. However, atherosclerosis should be considered to be a concomitant process and not a direct cause of aneurysm formation and growth. Aortic medial degeneration has been demonstrated in most aneurysms, regardless of their cause and location. In the ascending aorta, gradual degenerative changes of the media can be related to congenital disorders of the extracellular matrix associated with an alteration of the elastic fibers such as Marfan syndrome (Fig. 14). Moreover, families with a genetic predisposition to the development of thoracic and abdominal aneurysms, without evidence of collagen-vascular disease, have also been documented.

The estimated 5-year risk of rupture of a thoracic aneurysm with a diameter between 4 and 5.9 cm is 16%, but it rises to 31% for aneurysms of 6 cm or more. Because the only well-documented risk factor for aortic rupture is the increasing size of the aneurysm, the major goal in the imaging evaluation of an aortic aneurysm is accurate mea-

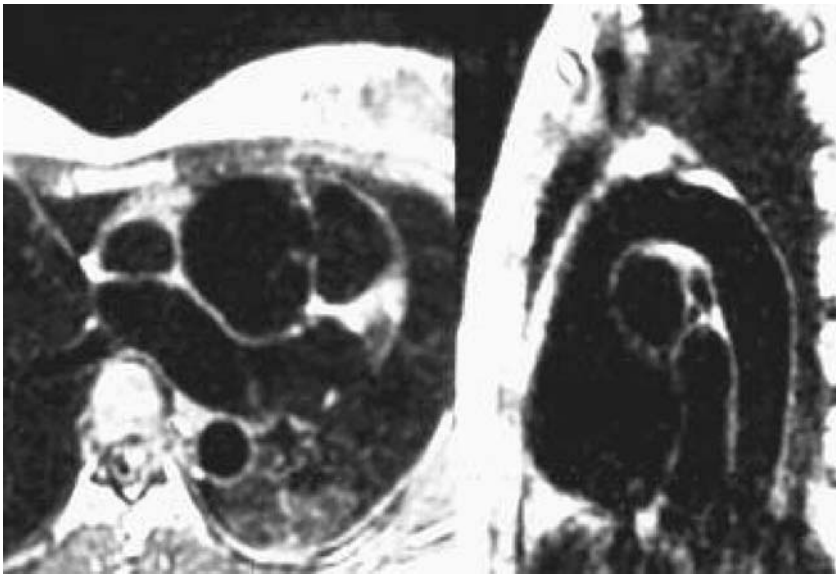

**Fig. 14** Spin-echo axial and sagittal images of the thoracic aorta of a Marfan patient: severe dilation of the Valsalva sinuses

surement of its size [54] and the monitoring of its evolution between two subsequent examinations.

MRI is effective in identifying and characterizing thoracic and abdominal aortic aneurysms. Standard spin-echo sequences are helpful in evaluating alterations of the aortic wall and periaortic space (Fig. 15). Periaortic hematoma and areas of high signal intensity within the thrombus may indicate instability of the aneurysm and are well depicted on spin-echo images. Atherosclerotic lesions are visualized as areas of increased thickness with high signal intensity and irregular profiles. Use of the sagittal plane allows the assessment of location and extent of the aneurysm and avoids partial volume effects. With fat suppression techniques, the outer wall of the aneurysm can be easily distinguished on MR images by the periadventitial fat tissue, allowing the aneurysm diameter to be accurately measured. The high level of reproducibility of MRI measurements ensures optimal reliability in monitoring expansion rate [49]. Gadolinium-enhanced T1-weighted MRI and MRA may play an important role in preoperative evaluation. Contrast-enhanced 3D MRA can provide precise topographic information about the extent of an aneurysm and its relationship to the aortic branches (Fig. 16) [11, 14, 16, 18]. The homogeneous enhancement of flowing blood within the lumen facilitates the delineation of thrombus.

As reported in the literature, the capability of contrast MRA to visualize the Adamkiewicz artery represents an important advance in planning the surgical repair of a thoracic aneurysm, thereby avoiding postoperative neurological deficit secondary to spinal cord ischemia [55].

## Aortic trauma

A traumatic aortic rupture is a lesion caused by trauma that extends from the intima to the adventitia. Trauma is the third leading cause of death in the United States and the leading cause of death in individuals under the age of 40.

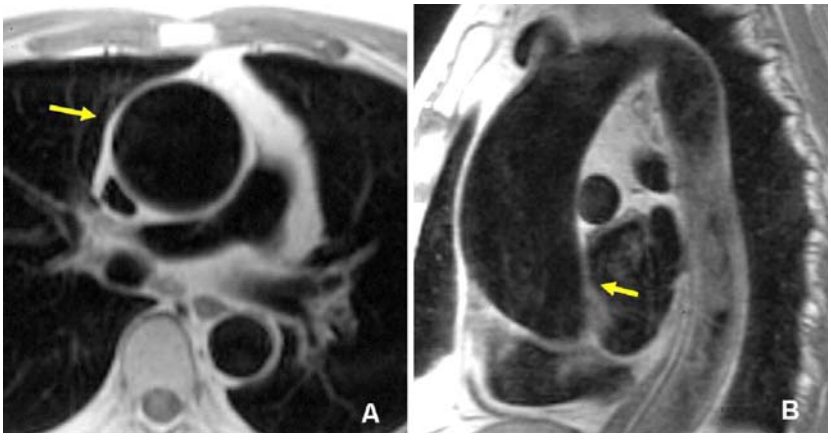


**Fig. 15** Axial and sagittal spin-echo images showing a dilated ascending aorta (*arrows*)

**Fig. 16** MRA image showing a dilated aortic root

**Fig. 17** Spin-echo sagittal image of acute traumatic aortic lesion: partial laceration of the aortic wall results in a diverticular aneurysm

Air bags and seatbelts do not protect against this type of injury, which is expected to increase in the statistics of road traffic injuries. The aortic segment subjected to the greatest strain by rapid deceleration forces is just beyond the isthmus. In clinical series, aortic rupture occurs 90% of the time at this site. Other less common sites are the distal ascending aorta, distal segments of the descending aorta, or the abdominal infrarenal segment. The lesion is transverse and involves all or part of the aortic circumference, penetrating the aortic layers to various degrees with the formation of a false aneurysm. Intimal hemorrhage without any laceration has been described in pathologic series but was not recognized in the clinical setting before the advent of high-resolution tomographic imaging modalities. Periaortic hemorrhage occurs irrespective of the type of lesion.

A long examination time as well difficult access to the patient have been considered to be the main limitations of MRI in acute aortic pathology. The development of fast MRI techniques have shortened the examination time to a few minutes, therefore MRI can even be used in critically ill patients. The value of MRI in detecting traumatic aortic rupture in comparison to angiography and conventional CT was reported in a series of 24 consecutive patients [56]. The potential for MRI to detect the hemorrhagic component of a lesion by its high signal intensity is beneficial in traumatized patients. On spin-echo images in the sagittal plane (Fig. 17), a longitudinal visualization of the thoracic aorta makes it possible to distinguish a partial lesion (a tear limited to the anterior or the posterior wall) from a lesion encompassing the entire aortic circumference. This discrimination is of prognostic significance because a circumferential lesion may be more likely to rupture [57]. The presence of periadventitial hematoma and/or pleural and mediastinal hemorrhagic effusion may also be considered a sign of instability. In the same sequence used to evaluate the aortic lesion, without the need of any additional time, the wide field of view of MRI provides a comprehensive evaluation of chest trauma such as lung contusion and

**Fig. 18** MR angiography of traumatic aortic lesion: the relationship with arch vessels is well depicted

edema, and pleural effusion and rib fractures. Furthermore, if delayed surgery is considered, MRI may be used to monitor thoracic and aortic lesions because it is noninvasive and repeatable.

MRA provides an excellent display of the aortic lesion and its relationship with supraaortic vessels (Fig. 18). However, it does not add any diagnostic value to spin-echo MRI, and it cannot supply information on parietal lesions and hemorrhagic fluids outside the aortic vessel.

## Aortitis

Inflammatory diseases of the aorta can be classified into two major subgroups: aortitis of nonspecific or unknown etiology (Takayasu aortitis, Bechet disease, giant cell aortitis, Kawasaki disease, ankylosing spondylitis), and specific aortitis, in which the aortitis is the consequence of an inflammatory disease of known origin (e.g., syphilitic aortitis). Relevant ethnic differences have been observed in the epidemiological distribution of nonspecific aortitis. They are common in Asian countries and rare in Caucasian populations, therefore the hypothesis of a genetic transmission is supported. Histologically, marked irregular mural thickening of the aortic wall and a fibrous lesion are the result of the inflammatory process of the media which can lead to stenotic lesions (Takayasu disease), aneurysms of the aorta and its major branches, or aortic insufficiency as a consequence of dilation of the aortic root.

The diagnosis of aortitis is often difficult because nonspecific systemic symptoms are present in the early phase when medical treatment may be more effective. Conventional angiography provides information mainly on the late manifestations of the disease such as vascular stenosis or localized aneurysms.

Contrast-enhanced T1- and T2-weighted spin-echo MRI has been shown to be highly effective in the evaluation of Takayasu arteritis [58], even in the early phases, providing important information on the activity of the disease. Active inflammatory disease appears as variable thickening of the aortic wall, enhanced after gadolinium administration as shown by Choe et al. [58] who reported 88% of concordance between contrast-enhanced MRI and clinical and laboratory findings in 26 patients with active Takayasu arteritis. The chronic, quiescent stage, however, is characterized by extensive perivascular fibrosis without contrast enhancement. High signal intensity of the aortic wall has been observed in giant cell aortitis, whereas media with fibrotic replacement generally has lower signal intensity. MRA can replace invasive angiography in the study of aortic and branch vessel stenosis, [59] and avoidance of angiography is highly desirable in patients affected by aortitis because it carries a risk of pseudoaneurysm formation at the site of arterial puncture. Recently, the capability of F-18 FDG hybrid camera PET combined with MRI to depict early stages of Takayasu aortitis [60, 61] has been demonstrated. Moreover, MRI can be useful in evaluating the response to medical treatment by depicting decreases in wall thickness of the involved arteries. A strict, life-long follow-up is therefore mandatory in patients with aortitis, both before and after surgery, because recurrence of the inflammatory process is frequently reported in patients who underwent surgery for aortitis, as is the risk of dehiscence of the sutures.

## MRI of human atherosclerotic plaque

Thoracic aortic atherosclerosis is a stronger predictor of coronary artery disease than conventional risk factors are, and it is also a marker of an increased risk for mortality, stroke, and visceral thromboembolic events. Autopsy studies, in fact, have shown that the amount of atherosclerotic plaque in the thoracic aorta correlates directly to the degree of atherosclerotic disease in the coronary arteries. MRI is a noninvasive imaging modality that can visualize and characterize the composition of atherosclerotic plaques and differentiates tissue structure on the basis of proton magnetic properties with an excellent soft tissue contrast [62–64]. High-resolution MRI has been increasingly used in assessing the vascular wall and characterizing atherosclerotic lesions [65]. The different composition of stable and unstable lesions can be discriminated by measuring T1, T2, and proton density changes [63]. Lipid components present hyperintense regions within the plaque on both T1- and proton density-weighted images and show a hypointense signal on T2-weighted images. Fibrocellular components are defined as hyperintense regions of the plaque on T1-, proton density-, and T2-weighted images. Calcium deposits can be appreciated as hypointense regions within the plaque on T1-, proton density- and T2-weighted images. The fibrous cap and lipid core, organized thrombus and fresh thrombosis or calcification and necrotic areas have been imaged in studies performed both in vitro and in vivo, and atherosclerotic lesions have been assessed in carotid arteries, coronary arteries and in the thoracic aorta. Direct, noninvasive assessment of aortic atherosclerotic plaque thickness, extent, and composition by MR, as already demonstrated in previous studies [66, 67], allows serial evaluation of the progression and therapy-induced regression of atherosclerotic plaques.

Another field of research in the atherosclerotic plaque evaluation is the development of MR contrast agents specific for plaque components like macrophages, fibrin, or lipids [68–70]. These contrast materials are captured by the plaque in a quantity sufficient for causing susceptibility effects detectable by MRI. Furthermore, carbon-13 MR spectroscopy can provide information on the chemical constituents of the lipid pool as a marker of the progression of the atherosclerotic plaque [71]. Another potential target for molecular MRI in atherosclerosis is the enzyme myeloperoxidase secreted by atherosclerotic inflammatory cells;

myeloperoxidase activity could be the perfect substrate for a dedicated contrast agent [72]. The advent of MR intravascular imaging devices further enhances the spatial resolution and homogeneity by providing close proximity between the imaging coil and the vessel wall [73]; the use of dedicated intravascular coils seems to increase MR performance in the atherosclerotic plaque evaluation [74]. The combination of tissue characterization and spectroscopy may have an extraordinary potential in assessing the characteristics of plaque, so that new insight into plaque formation and evolution will be acquired.

## Interventional MRI

In the era of minimally-invasive endovascular procedures like balloon angioplasty and stent implantation, there is an increasing interest in using MRI instead of X-ray fluoroscopy for the guidance and monitoring of these interventional vascular procedures. Magnetic resonance provides excellent contrast of vascular structures, especially between the lumen and the vessel wall, without radiation exposure of the patient and interventionists. With respect to catheter angiography, MRI can provide a complete evaluation of the interventional procedure in terms of morphology and hemodynamic significance using phase contrast sequences. The entire procedure could be adequately monitored by a near real-time (up to 1 image/s) MR fluoroscopy using a dynamic two dimensional fast gradient-echo technique with the possibility of a digital subtraction from a previously acquired mask. This technique needs dedicated materials (catheters, guidewires, etc.) prepared for susceptibility-based MR visualization by means of paramagnetic markers placed into their walls.

Some experimental in vitro and in vivo studies [75–77] assess the feasibility of this technique, even if is still too far from actual clinical practice, especially in interventional procedures which require general anesthesia and surgical support, like thoracic or abdominal aortic stent implantation.

To date, the limitations of interventional MRI are long procedure times, lack of true real-time monitoring, and stent artifacts, which necessitate further modifications before they can be recommended for clinical use. However, MRI-guided interventions are feasible and may become an important advancement in the near future.

## References


1. Urban BA, Bluemke DA, Johnson KM, Fishman EK (1999) Imaging of thoracic aortic disease. Cardiol Clin 17 (4):659–682
2. Reddy GP, Higgins CB (2000) MR imaging of the thoracic aorta. Magn Reson Imaging Clin N Am 8(1):1–15
3. Stemerman DH, Krinsky GA, Lee VS, Johnson G, Yang BM, Rofsky NM (1999) Thoracic aorta: rapid black-blood MR imaging with half-Fourier rapid acquisition with relaxation enhancement with or without electrocardiographic triggering. Radiology 213 (1):185–191
4. Sakuma H, Bourne MW, O'Sullivan M et al (1996) Evaluation of thoracic aortic dissection using breath-holding Cine MRI. J Comput Assist Tomogr 20 (1):45–50
5. Niezen RA, Doornbos J, van der Wall EE, de Roos A (1998) Measurement of aortic and pulmonary flow with MRI at rest and during physical exercise. J Comput Assist Tomogr 22(2): 194–201
6. Powell AJ, Maier SE, Chung T, Geva T (2000) Phase-velocity cine magnetic resonance imaging measurement of pulsatile blood flow in children and young adults: in vitro and in vivo validation. Pediatr Cardiol 21(2):104–110
7. Bogren HG, Buonocore MH (1999) 4D magnetic resonance velocity mapping of blood flow patterns in the aorta in young vs. elderly normal subjects. J Magn Reson Imaging 10(5):861–869
8. Hopkins KD, Leheman ED, Gosling RG (1994) Aortic compliance measurements: a noninvasive indicator of atherosclerosis. Lancet 334:1447
9. Groenink M, de Roos A, Mulder BJM, Spaan JAE, van der Wall EE (1998) Changes in aortic distensibility and pulse wave velocity assessed with magnetic resonance imaging following beta-blockers therapy in the Marfan syndrome. Am J Cardiol 82:203–208
10. Fattori R, Bacchi Reggiani L, Pepe G et al (2000) MRI evaluation of aortic elastic properties as early expression of Marfan Syndrome. J Cardiovasc Magn Reson 4:43–48
11. Debatin JF, Hany TF (1998) MR-based assessment of vascular morphology and function. Eur Radiol 8:528–539
12. Sodickson DK, McKenzie CA, Li W, Wolff S, Manning WJ, Edelman RR (2000) Contrast-enhanced 3D MR angiography with simultaneous acquisition of spatial harmonics: a pilot study. Radiology 217(1):284–289
13. Lee VS, Martin DJ, Krinsky GA, Rofsky NM (2000) Gadolinium-enhanced MR angiography: artifacts and pitfalls. Am J Roentgenol 175:197–205
14. Neimatallah MA, Ho VB, Dong Q et al (1999) Gadolinium-enhanced 3D Magnetic Resonance angiography of the thoracic vessels. JMRI 10:758–770
15. Goyen M, Ruehm SG, Debatin JF (2000) MR-angiography: the role of contrast agents. Eur J Radiol 34 (3):247–256
16. Prince MR, Narasimham DL, Jacoby WT et al (1996) Three dimensional Gadolinium-enhanced MR angiography of the thoracic aorta. Am J Roentgenol 166:1387–1397
17. Krinsky G, Rofsky N, Flyer M et al (1996) Gadolinium-enhanced three dimensional MR angiography of acquired arch vessels disease. Am J Roentgenol 167:981–987
18. Krinsky G, Rofsky N, De Corato DR et al (1997) Thoracic aorta: comparison of Gadolinium-enhanced three dimensional MR angiography with conventional MR imaging. Radiology 202:183–193
19. Riederer SJ, Bernstein MA, Breen JF, Busse RF, Ehman RL, Fain SB, Hulshizer TC, Huston J III, King BF, Kruger DG, Rossman PJ, Shah S (2000) Three-dimensional contrast-enhanced MR angiography with real-time fluoroscopic triggering: design specifications and technical reliability in 330 patient studies. Radiology 215:584–593

20. Coady MA, Rizzo JA, Goldstein LJ, Elefteriades JA (1999) Natural history, pathogenesis and etiology of thoracic aneurysms and dissection. Card Clin North Am 17(4):615–633
21. Bansal RC, Krishnaswamy C, Ayala K, Smith DC (1995) Frequency and explanation of false negative diagnosis of aortic dissection by aortography and transesophageal echocardiography. J Am Coll Cardiol 25:1393–401
22. Spittel PC, Spittel JA, Joyce W et al (1993) Clinical features and differential diagnosis of aortic dissection: experience with 236 cases (1980 through 1990). Mayo Clin Proc 68:642–651
23. Cigarroa JE, Isselbacher EM, De Sanctis RW, Eagle KA (1993) Diagnostic imaging in the evaluation of suspected aortic dissection: old standard and new direction. N Engl J Med 328:35–43
24. Nienaber CA, Fattori R, Lund G, Dieckman C, Wolf W, Nikolas V, Pierangeli A (1999) Nonsurgical reconstruction of thoracic aortic dissection by stent-graft placement. N Eng J Med 140:1338–1345
25. Dake MD, Kato N, Mitchell RS et al (1999) Endovascular stent-graft placement for the treatment of acute aortic dissection. N Engl J Med 140:1546–1552
26. Nitatori T, Yokoyama K, Hachiya J, Yoshino A, Yamakami N, Katase S, Ichikawa T (1999) Fast dynamic MRI of aortic dissection: flow assessment by subsecondal imaging. Radiat Med 17 (1):9–14
27. Chang JM, Friese K, Caputo GR, Kondo C, Higgins CB (1991) MR measurement of blood flow in the true and false channel in chronic aortic dissection. J Comput Assist Tomogr 15:418–423
28. Fernandez GC, Tardaguila FM, Duran D, Trinidad C, Rodriguez M, Hortas M (2002) Dynamic 3-dimensional contrast-enhanced magnetic resonance angiography in acute aortic dissection. Curr Probl Diagn Radiol 31(4): 134–145
29. Bogaert J, Meyns B, Rademakers FE et al (1997) Follow-up of aortic dissection: contribution of MR angiography for evaluation of the abdominal aorta and its branches. Eur Radiol 7:695–702
30. Nienaber CA, von Kodolitsch Y, Nikolas V et al (1993) The diagnosis of thoracic aortic dissection by noninvasive imaging procedures. N Engl J Med 328:1–9
31. Sommer T, Fehske W, Holzknecht et al (1996) Aortic dissection: a comparative study of diagnosis with spiral CT, multiplanar transesophageal echocardiography and MR imaging. Radiology 199:347–352
32. Fisher U, Vossherich R, Kopka L, Keating D, Oestmann J, Grabbe E (1994) Dissection of the thoracic aorta: pre- and postoperative findings of turbo-FLASH MR images in the plane of the aortic arch. Am J Roentgenol 163:1069–1072
33. Krukemberg E (1920) Beiträge zur Frage des Aneurysma dissecans. Beitr Pathol Anat Allg Pathol 67:329–351
34. Fattori R, Bertaccini P, Celletti F et al (1997) Intramural post-traumatic hematoma of the ascending aorta in a patient with a double aortic arch. Eur Radiol 7:51–53
35. Nienaber CA, von Kodolitsch Y, Petersen B et al (1995) Intramural hemorrhage of the thoracic aorta: diagnostic and therapeutic implication. Circulation 92:1465–1472
36. Coady MA, Rizzo JA, Elefteriades JA (1999) Pathologic variants of thoracic aortic dissections: penetrating atherosclerotic ulcers and intramural hematomas. Cardiol Clin 17(4):637–657
37. Yamada T, Takamiya M, Naito H, Kozuka T, Nakajima N (1985) Diagnosis of aortic dissection without intimal rupture by X-ray computed tomography. Nippon Igaku Hoshasen Gakkai Zasshi 45(5):699–710
38. Moore A , Oh J, Bruckman D et al (1999) Transesophageal echocardiography in the diagnosis and management of aortic dissection: an analysis of data from the International Registry of Aortic Dissection (IRAD). J Am Coll Cardiol 33–2(A):470A
39. Murray JG, Manisali M, Flamm SD et al (1997) Intramural hematoma of the thoracic aorta: MR imaging findings and their prognostic implications. Radiology 204:349–355
40. Shennan T (1934) Dissecting aneurisms. Medical Research Council Special Report series no. 193, Medical Research Council, London
41. Movsowitz HD, Lampert C, Jacobs LE, Kotler MN (1994) Penetrating atherosclerotic aortic ulcers. Am Heart 128:1210–1217
42. Hayashi H, Matsuoka Y, Sakamoto I, Sueyoshi E, Okimoto T, Hayashi K, Matsunaga N (2000) Penetrating atherosclerotic ulcer of the aorta: imaging features and disease concept. Radiographics 20(4):995–1005
43. Yucel EK, Steinberg FL, Egglin TK, Geller SC, Waltman AC, Athanasoulis CA (1990) Penetrating atherosclerotic ulcers: diagnosis with MR imaging. Radiology 177:779–781
44. Fann JI, Smith JA, Miller CD et al (1995) Surgical management of aortic dissection during a 30 year period. Circulation 92(suppl II):110–121
45. Svensson LG, Crawford SE (1997) Statistical analyses of operative results. In: Cardiovascular and vascular disease of the aorta. Saunders, Philedelphia, pp 432–455
46. Fattori R, Bacchi Reggiani ML, Bertaccini P et al (2000) Evolution of aortic dissection after surgical repair. Am J Cardiol 86(8):868–872
47. Moore NR, Parry AJ, Trottman-Dickenson B, Pillay R, Westaby S (1996) Fate of the native aorta after repair of acute type A dissection: a magnetic resonance imaging study. Heart 75:62–66
48. Mesana TG, Caus T, Gaubert J, Collart F, Ayari R, Bartoli J, Moulin G, Monties J (2000) Late complications after prosthetic replacement of the ascending aorta: What did we learn from routine magnetic resonance imaging follow-up? Eur J Cardio-Thorac Surg 18(3):313–320
49. Kawamoto S, Bluemke DA, Traill TA, Zerhouni EA (1997) Thoracoabdominal aorta in Marfan syndrome: MR Imaging findings of progression of vasculopathy after surgical repair. Radiology 203:727–732
50. Gaubert J, Moulin G, Mesana T et al (1995) Type A dissection of the thoracic aorta: use of MR imaging for long term follow-up. Radiology 196: 363–369
51. Loubeyre P, Delignette A, Boneloy L, Douek P, Amiel M, Revel D (1996) MRI evaluation of the ascending aorta after graft-inclusion surgery: comparison between an ultra-fast contrast-enhanced MR sequence and conventional cine-MRI. JMRI 6: 478–483
52. Fattori R, Descovich B, Bertaccini P et al (1999) Composite graft replacement of the ascending aorta: leakage detection with gadolinium-enhanced MR imaging. Radiology 212:573–577
53. Clouse WD, Hallett JW, Shaff HV, Gayari MM, Ilstrup DM, Melton LJ III (1998) Improved prognosis of thoracic aortic aneurysm: a population based study. JAMA 9(280):1926–1929
54. Bonser RS, Pagano D, Lewis ME, Rooney SJ, Guest P, Davies P, Shimada I (2000) Clinical and patho-anatomical factors affecting expansion of thoracic aortic aneurysms. Heart 84(3):277–283

55. Yamada N, Okita Y, Minatoya K et al (2000) Preoperative demonstration of the Adamkiewicz artery by magnetic resonance angiography in patients with descending or thoracoabdominal aortic aneurysms. Eur J Cardio-Thorac Surg 18(1):104–111
56. Fattori R, Celletti F, Bertaccini et al (1996) Delayed surgery of traumatic aortic rupture: role of magnetic resonance imaging. Circulation 94:2865–2870
57. Fattori R, Celletti F, Descovich B et al (1998) Evolution of post traumatic aneurysm in the subacute phase: magnetic resonance imaging follow-up as a support of the surgical timing. Eur J Cardio-Thorac Surg 13:582–587
58. Choe YH, Kim DK, Koh EM, Do YS, Lee WR (1999) Takayasu arteritis: diagnosis with MR imaging and MR angiography in acute and chronic active stages. J Magn Reson Imaging 10 (5):751–757
59. Berkmen T (1999) MR Angiography of aneurysms in Beçhet disease: a report of four cases. J Comput Assist Tomogr 1998:202–206
60. Meller J, Grabbe E, Becker W, Vosshenrich R (2003) Value of F-18 FDG hybrid camera PET and MRI in early Takayasu aortitis. Eur Radiol 13 (2):400–405
61. Vanderschueren S, Buysschaert I, Mortelmans L, Blockmans D, Knockaert DC (2004) Comment on Meller et al.: value of F-18 FDG hybrid camera PET and MRI in early Takayasu aortitis. Eur Radiol 14(5):926–929. Author reply 928–929
62. Fayad ZA, Fallon JT, Shinnar M et al (1998) Noninvasive in vivo high resolution magnetic resonance imaging of atherosclerotic plaque in genetically engineered mice. Circulation 98: 1541–1547
63. Leiner T, Gerretsen S, Botnar R, Lutgens E, Cappendijk V, Kooi E, van Engelshoven J (2005) Magnetic resonance imaging of atherosclerosis. Eur Radiol 15(6):1087–1099
64. Fayad ZA, Nahar T, Fallon JT et al (2000) In vivo magnetic resonance evaluation of atherosclerotic plaques in the human thoracic aorta: a comparison with transesophageal echocardiography. Circulation 101(21):2503–2509
65. Worthley SG, Helft G, Fuster V, Zaman AG, Fayad ZA, Fallon JT, Badimon JJ (2000) Serial in vivo MRI documents arterial remodeling in experimental atherosclerosis. Circulation 101 (6):586–589
66. Fayad ZA, Nahar T, Fallon JT, Goldman M, Aguinaldo JG, Badimon JJ, Shinnar M, Chesebro JH, Fuster V (2000) In vivo magnetic resonance evaluation of atherosclerotic plaques in the human thoracic aorta: a comparison with transesophageal echocardiography. Circulation 101(21):2503–2509
67. Chan SK, Jaffer FA, Botnar RM, Kissinger KV, Goepfert L, Chuang ML, O'Donnell CJ, Levy D, Manning WJ (2001) Scan reproducibility of magnetic resonance imaging assessment of aortic atherosclerosis burden. J Cardio vasc Magn Reson 3(4):331–338
68. Ruehm SG, Corot C, Vogt P, Kolb S, Debatin JF (2001) Magnetic resonance imaging of atherosclerotic plaque with ultrasmall superparamagnetic particles of iron oxide in hyperlipidemic rabbits. Circulation 103(3):415–422
69. Schmitz SA, Taupitz M, Wagner S, Wolf KJ, Beyersdorff D, Hamm B (2001) Magnetic resonance imaging of atherosclerotic plaques using superparamagnetic iron oxide particles. J Magn Reson Imaging 14(4):355–361
70. Yu X, Song SK, Chen J, Scott MJ, Fuhrhop RJ, Hall CS, Gaffney PJ, Wickline SA, Lanza GM (2000) High-resolution MRI characterization of human thrombus using a novel fibrin-targeted paramagnetic nanoparticle contrast agent. Magn Reson Med 44 (6):867–872
71. Toussaint J, Southern JF, Fuster V, Kantor HL (1994) $^{13}$-NMR spectroscopy of Human atherosclerotic lesions: relation between fatty acid saturation, cholesteryl ester content and luminal obstruction. Circulation 14: 1951–1957
72. Chen JW, Pham W, Weissleder R, Bogdanov A Jr (2004) Human myeloperoxidase: a potential target for molecular MR imaging in atherosclerosis. Magn Reson Med 52(5):1021–1028
73. Zimmermann-Paul GG, Quick HH, Vogt P, von Schulthess GK, King D, Debatin JF (1999) High resolution intravascular magnetic resonance imaging: monitoring of plaque formation in heritable hyperlipidemic rabbits. Circulation 99:1054–1061
74. Farrar CT, Wedeen VJ, Ackerman JL (2005) Cylindrical meanderline radiofrequency coil for intravascular magnetic resonance studies of atherosclerotic plaque. Magn Reson Med 53 (1):226–230
75. Glowinski A, Adam G, Bucker A, Neuerburg J, van Vaals JJ, Gunther RW (1997) Catheter visualization using locally induced, actively controlled field inhomogeneities. Magn Reson Med 38(2):253–258
76. Bakker CJ, Smits HF, Bos C, van der Weide R, Zuiderveld KJ, van Vaals JJ, Hurtak WF, Viergever MA, Mali WP (1998) MR-guided balloon angioplasty: in vitro demonstration of the potential of MRI for guiding, monitoring, and evaluating endovascular interventions. J Magn Reson Imaging 8(1):245–250
77. Godart F, Beregi JP, Nicol L, Occelli B, Vincentelli A, Daanen V, Rey C, Rousseau J (2000) MR-guided balloon angioplasty of stenosed aorta: in vivo evaluation using near-standard instruments and a passive tracking technique. J Magn Reson Imaging 12(4):639–944